Martian geomorphology from fractal analysis of drainage networks

T. F. Stepinski
Lunar and Planetary Institute, Houston, Texas, USA

M. L. Collier
Department of Earth Science, Rice University, Houston, Texas, USA

P. J. McGovern and S. M. Clifford
Lunar and Planetary Institute, Houston, Texas, USA

Received 30 March 2003; revised 27 October 2003; accepted 17 November 2003; published 19 February 2004.

[1] An alternative approach to conventional planetary terrain analysis is proposed. Martian terrains, represented by topography based on the Mars Orbiter Laser Altimetry (MOLA) data, are represented as a series of drainage basins, regardless of the historical presence or absence of actual fluid flow. A fractal analysis of each drainage network, computationally extracted from an underlying terrain, yields a network descriptor, a list of four numbers that describes the traits of a network. Network descriptors are used for a quantitative characterization and classification of Martian surfaces. We have extracted and analyzed 387 drainage networks from 74 Martian locations, representing all major epochs and geological units, to investigate whether their network descriptors are capable of differentiation between different epochs and geological units. We have found that our approach can distinguish morphologically different terrains, but only in a statistical sense. In particular, the method could be used to measure the degree of surface cratering and thus the age of the surface. In addition, for surfaces that are not heavily cratered the method is capable of distinguishing between different geological units. We have found no global trends in the character of Martian drainage networks; their network descriptors show no systematic dependence on location or elevation. Our analysis reveals that all Noachian surfaces grouped in the Npld geological unit have very similar network descriptors, regardless of prominence and integration of their visible fluvial features. The comparison between statistical description of Npld and terrestrial drainage networks shows overall similarities, but also some marked differences. Because of these differences, the notion of sustained rainfall on Mars during the Noachian epoch is inconsistent with our findings, but a limited rainfall is compatible with our results. *INDEX TERMS:* 3250 Mathematical Geophysics: Fractals and multifractals; 1824 Hydrology: Geomorphology (1625); 1848 Hydrology: Networks; 5415 Planetology: Solid Surface Planets: Erosion and weathering; 6225 Planetology: Solar System Objects: Mars; *KEYWORDS:* erosion, Mars, mathematical geophysics, weathering

Citation: Stepinski, T. F., M. L. Collier, P. J. McGovern, and S. M. Clifford (2004), Martian geomorphology from fractal analysis of drainage networks, *J. Geophys. Res.*, *109*, E02005, doi:10.1029/2003JE002098.

1. Introduction

[2] Morphology of Martian landscapes is of great interest because it helps to identify physical processes responsible for the presently observable topography. For example, some portions of the Martian surface show features reminiscent of terrestrial river networks, possibly formed by rainfall-fed fluvial erosion [*Pieri*, 1980; *Carr and Clow*, 1981; *Craddock and Maxwell*, 1993]. The positive identification of rainfall-fed fluvial erosion as the mechanism responsible for the observed topographical features is important inasmuch as it would indicate an existence of the warm period in Mars' past.

0148-0227/04/2003JE002098$09.00

[3] Traditionally, the descriptive morphology has been used to study and categorize different types of Martian landscapes. Using natural language to characterize landscapes was dictated by the fact that the raw data were provided in the form of images, and because landscapes are complex objects that are hard to describe in terms of a quantitative and formalized system. Currently, the Mars Orbiter Laser Altimeter (MOLA) data can be utilized to provide a full topographical description of any given Martian terrain. Digital elevation models (DEMs) constructed from the MOLA data are suitable for a quantitative analysis. A DEM is a regular rectangular grid of sites for which elevations are assigned. In order to be useful, the quantitative analysis of a terrain, as represented by a DEM,

requires an extensive "compression" of the data so the result has a relatively simple interpretation and can be used for characterization and categorization of a given terrain. Note that the traditional, qualitative morphology also uses massive "data compression" as only the global character of what appears in an image, and not the total content of all the individual pixels, is reflected in a description.

[4] We propose that a drainage network, overlaying a given terrain, constitutes a convenient compression of the entire topographical information contained in this terrain. Although the network does not uniquely determine the terrain, it nevertheless, reflects its general character. Thus we submit that a quantitative comparison of drainage networks is tantamount to a quantitative comparison of landscapes. It is important to stress that a "drainage network" can be computationally extracted from any terrain, including terrains that never experienced any real flow. Recently, *Stepinski et al.* [2002] applied this idea to show that drainage networks extracted from Martian, terrestrial, and lunar landscapes are all statistically different from each other. Drainage networks from a particular planet have characteristic properties that reflect the morphology of an underlying landscape and thus the physical process responsible for this morphology. Terrestrial networks carry properties that can be assigned to the process of rainfall-fed fluvial erosion, while lunar networks carry properties that can be assigned to the process of erosion by bombardment. Selected Martian networks studied by *Stepinski et al.* [2002] have their own characteristic properties interpreted as arising from the mixture of fluvial erosion and bombardment.

[5] Comparative geomorphology of landscapes based on the Drainage Network Analysis (DNA) constitutes an algorithmic, quantitative, and objective method that supplements traditional, descriptive method and may provide new insights. The purpose of this paper is to study the suitability of the DNA method for various problems in Martian geomorphology. We concentrate exclusively on Martian landscapes. In particular, we are interested whether the DNA method is sensitive to the age of the terrain and whether it can recognize geological units.

2. Methods

[6] The input data for our analysis are from a DEM of a Martian landscape. The DNA method consists of two stages, obtaining a drainage network and then analyzing it. A drainage network is computationally extracted from a DEM using an algorithm developed for studies of terrestrial river basins [*Tarboton et al.*, 1989]. As the first step, the algorithm modifies the DEM by making it "drainable" by "flooding" all pits in the digital representation of the terrain. Terrestrial terrains are naturally drainable, so flooded pits are usually data anomalies. However, Martian surfaces contain natural pits, such as craters. The flooding converts craters into "lakes," and the topographical information inside the craters is lost. However, because "lakes" drain in a very specific, algorithm assigned pattern, the DNA method readily identifies cratered surfaces. In the second step, each site in the modified DEM is assigned a drainage pointer to a neighbor site in the direction of the steepest slope. Using drainage directions, the total contributing area, a, is calculated for each site in a DEM. This quantity is the total number of sites draining into a given site, and is also a measure of the flow rate through that site. Finally, the drainage network is defined as collection of sites with $a \geq a_{ch}$. In the context of terrestrial hydrology a_{ch} is a proxy for a minimum flow that causes channelization and its value can be determined objectively [*Tarboton et al.*, 1991]. However, in our present context a_{ch} is a free parameter, a drainage network extends to smaller scales for smaller values of a_{ch}. In hydrology getting the right value of a_{ch} is important because the goal is to get an extracted network to be as close as possible to the actual river network. In our DNA method a network is a compact representation of a landscape and no specific value of a_{ch} is preferred. It turns out that extracted networks have all fractal geometry, and thus their properties are scale-invariant, at least for some range of a_{ch} values. In our calculations we use $a_{ch} = 60$.

[7] An extracted network has a spanning tree geometry and terminates in an outlet. The branching hierarchy of a network is described by the Horton-Strahler order denoted by Ω (see *Rodriguez-Iturbe and Rinaldo* [1997] and *Dodds and Rothman* [2000] for details). Extensive phenomenological studies [*Horton*, 1945; *Hack*, 1957; *Tarboton et al.*, 1988] of terrestrial drainage networks (representing landscapes evolved by rainfall-fed fluvial erosion) showed that their structure is fractal [*Rodriguez-Iturbe and Rinaldo*, 1997; *Rinaldo et al.*, 1998]. All of the networks we have extracted from Martian landscapes are also fractals as corroborated by power law distributions of several drainage quantities (see below).

[8] The second stage of our DNA method is to categorize fractal networks, using methods originally developed for terrestrial hydrology [*Rodriguez-Iturbe and Rinaldo*, 1997; *Rinaldo et al.*, 1998]. We describe networks in terms of probability distribution functions (PDFs) of drainage quantities defined at any point S on a network. Such a statistical description has an advantage of exposing the universality of drainage networks. Two networks extracted from landscapes of the same origin may "look" very different, but their statistical properties are similar. Such an universality has been demonstrated for a number of artificially constructed landscapes (see *Dodds and Rothman* [2000] for a review) and for terrestrial river networks. Thus, in our DNA method the statistics of drainage quantities constitute the fingerprints of a landscape. Following *Stepinski et al.* [2002], we describe the network by statistical properties of the following drainage quantities: a, a previously defined total contributing area at S; l, length of the longest upstream path starting from S; and e, dissipated potential energy, a product of the flow and the elevation rise along a segment of the network terminating at S. Empirical cumulative distribution functions (CDFs) of these quantities, plotted on the logarithnic scale, exhibit linear dependence over significant portions of quantities' ranges. This indicate that the PDFs of these quantities are power laws, $P(a) \propto a^{-(1+\tau)}$, $P(l) \propto l^{-(1+\gamma)}$, $P(e) \propto e^{-(1+\beta)}$, and a given network can be statistically characterized by the power law indices τ, γ, and β.

[9] The indices τ and γ pertain to the planar character of the network, while β pertains to the vertical structure of the network. Comparing two networks with $\tau_1 > \tau_2$, the first network has a higher proportion of small to large subbasins; thus it is organized in a more hierarchical fashion. Similar interpretation can be given to the relative values of

γ and β. Note that τ and γ are not independent. It is intuitive to expect that regardless of the character of a network, the length of a given basin's main stream l and a basin area a are related. Assuming that such a relation can be described as $l \propto a^h$, it can be shown [*Dodds and Rothman*, 2000] that $\tau/\gamma = h$. In principle the value of h may change from one network to another, but for terrestrial networks, the value of h is approximately the same for all networks ($h_{\text{terr}} \approx 0.6$) and the relation $l \propto a^h$, one of the commonest empirical laws in geomorphology, is called Hack's law [*Hack*, 1957]. The existence of Hack's law reflects an organization of a landscape in response to an erosive mechanism: rainfall-fed fluvial erosion. A high correlation between τ and γ for networks extracted from a Martian terrain would also indicate landscape organization in reaction to a single, predominate erosion mechanism. In addition, the value of h close to h_{terr} suggests (but does not prove) that the landscape organizing mechanism is the rainfall-fed fluvial erosion. To calculate values of τ, γ, and β for a given network, we construct empirical CDFs of quantities a, l, and e, respectively, using their values at the nodes of the network. Values of the exponents τ, γ, and β are estimated by a least-squares power law fit to the respective empirical CDFs. The quality of the fit is very good for distributions of τ and γ, with a typical value of reduced χ^2 equal to 0.5. The quality of the fit for distribution of β is fair with a typical value of reduced χ^2 equal to 1.0.

[10] In addition, a drainage density, D, is defined for a sub-basin terminating at S and measures the average area drained per unit length of stream. Because in the DNA method the extent of a network depends on an assumed value of a_{ch}, we cannot unambiguously calculate the value of D, however we can calculate ρ, the ratio of the mean to the dispersion of the random variable D. The quantity ρ measures the uniformity of D and is independent from the assumed value of a_{ch}. Large values of ρ indicate high uniformity of D. A basin characterized by a high value of ρ contains a homogeneous terrain, that usually (but not always) is a highly eroded surface. Small value of ρ characterizes a basin with an uneven drainage density and usually points to a rough, uneroded terrain. The value of ρ is calculated directly from the data at the nodes of the network.

[11] A morphology of a given network, and thus the morphology of an underlying landscape, can be encapsulated in a list, A, of four numbers $A = (\tau, \gamma, \beta, \rho)$ which we call the network descriptor. In our study several networks are extracted from a landscape of interest and the network descriptor, A, is calculated for every network. The goal of the DNA method is to use the network descriptor as a quantitative and objective tool to characterize and categorize Martian landscapes, and to link, in a statistical sense, the nature of a surface to the process by which it has formed.

3. Data

[12] In order to sample a wide range of Martian landscapes, we have chosen 74 locations from around the Martian globe to represent all three major epochs and 16 geological units, as identified by *Scott and Carr* [1977]. In addition, care was taken to select terrains from a wide range of latitudes and elevations. The topography of the terrains was extracted from the MOLA global topographic model grid [*Smith et al.*, 2001], which currently has resolution of 1/128 degree in both latitude and longitude. Topography data were projected into a rectilinear coordinate system and assigned to 500-m square bins using the "surface" adjustable tension continuous curvature gridding algorithm of the Generic Mapping Tools (GMT) software package [*Wessel and Smith*, 1991]. Together, the analyzed areas cover ~3% of the Martian surface, and the sampled geological units are representative of ~50% of the planet. Using these DEMs, we have extracted 387 drainage networks spanning basins with the combined area of ~1.5% of the Martian surface. For each network a number of properties was calculated including the network descriptor A, creating a database to be used in our analysis.

[13] Extracted Martian networks span basins ranging in size from 2.5×10^4 km^2 with the drainage network of 7879 links having a Horton-Strahler order of $\Omega = 6$, to 4.0×10^2 km^2 with the drainage network of just 13 links having Horton-Strahler order of $\Omega = 2$. There are 152 networks extracted from Noachian surfaces, 145 from Hesperian, and 89 from Amazonian. Network outlets are chosen randomly, but in the cases where a landscape has a visual valley networks, an extracted network follows it closely.

4. Terrains of Different Ages

[14] We investigate whether the DNA method is capable of distinguishing between terrains of different ages. All extracted networks have been divided into three age-related categories, Noachian, Hesperian, and Amazonian. For each category we have estimated the PDFs of τ, γ, β, and ρ, using the method described by *Gershenfeld* [1999]. Figure 1 shows the result. It appears that networks quantities from different Martian epochs are, nevertheless, distributed in a very similar fashion. All quantities have a gaussian-like distributions with respective values of the mean and the standard deviation that are given in Table 1. Comparing the average values of A does not provide a clear statistical distinction between different Martian epochs, the way it provided a distinction between terrestrial, lunar, and Martian surfaces in the study by *Stepinski et al.* [2002].

[15] In addition to calculating the distributions of individual components of A, we have also investigated the overall distribution of A in a four-dimensional space. The network descriptor A is divided into two subsets, (τ, γ) and (ρ, β). Such a split is warranted because the first pair, (τ, γ), ties together the two planar characteristics of the network. The remaining pair, (ρ, β), combines quantities that pertain to the degree of a potential fluvial erosion of a surface.

[16] Figure 2 shows the $\tau - \gamma$ and $\rho - \beta$ diagrams for networks extracted from Noachian, Hesperian, and Amazonian terrains, respectively. Comparing $\tau - \gamma$ diagrams for different epochs it is clear that a correlation between τ and γ sharply increases for progressively younger terrains. For networks extracted from Noachian terrains the correlation coefficient for τ and γ is $r_{\text{Noach}} = 0.25$, but for networks extracted from Hesperian terrains $r_{\text{Hes}} = 0.61$, and for networks extracted from Amazonian terrains $r_{\text{Am}} = 0.7$. Therefore the degree of correlation between τ and γ appears to be an indicator of surface age.

[17] We explain this trend as follows. For Martian surfaces, the crater count provides a measure of the age of a

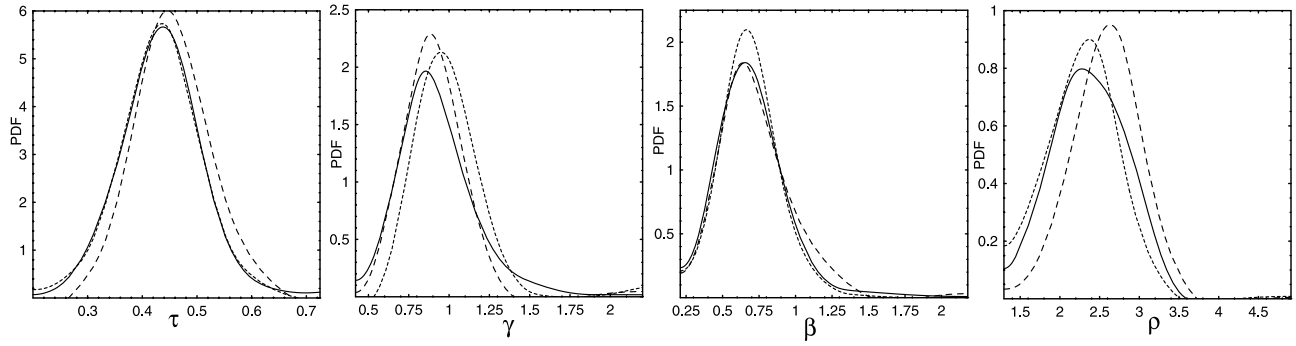

Figure 1. Distributions of values of individual drainage quantities constituting the network descriptor for Martian terrains of different ages. The panels from left to right show PDFs of τ, γ, β, and ρ, respectively. Short-dashed curves correspond to Noachian terrains, solid curves to Hesperian terrains, and long-dashed curves to Amazonian terrains.

surface, older surfaces being more cratered than the younger ones. In a collection of networks with outlets chosen at random locations, extracted from a heavily cratered surface, some networks happen to incorporate a crater (or multiple craters), while others happen to avoid any craters. Because planar characters of networks depend on the embodiments of craters into their structures, the extracted networks have a broad range of properties resulting in a low correlation between τ and γ. On the other hand, networks extracted from a surface with a low crater count are not likely to pass through craters, thus their properties are not subject to perturbations caused by the random embodiment of craters. In such a case the scatter in network properties is only due to intrinsic variations in a erosional process, and, as discussed in section 2, a high correlation between τ and γ is expected.

[18] We fit a linear relation to (τ, γ) data; the best fits are indicated by dashed lines in Figure 2. The inverse of the best-fit line's slope can be associated with an index h in "Hack's law" (see section 2). We have obtained $h_{\mathrm{Noach}} = 1.35$, $h_{\mathrm{Hes}} = 0.52$, and $h_{\mathrm{Am}} = 0.48$. However, a validity of a linear fit approximation, and thus an existence of single, universal value of h for all networks in a sample, holds only for the data where τ and γ are significantly correlated. Thus the Noachian data are too scattered to be described satisfactorily by a single value of h, whereas a single value of h makes sense for the Amazonian data. In cases where it is well defined, the parameter h controls a shape of drainage basin relative to a shape of its component sub-basins. For $h = 0.5$ a basin and its sub-basins have all the same shape (in a statistical sense), for $h > 0.5$ a basin has a more elongated shape than its sub-basins, and for $h < 0.5$ the sub-basins are more elongated than a parent basin. A familiar structure of terrestrial drainage basins, with basins more elongated than their sub-basins, corresponds to $h_{\mathrm{terr}} \approx 0.6$. Interestingly, $h_{\mathrm{Am}} \leq 0.5$ points to a fundamental difference between internal organizations of terrestrial and Amazonian drainage basins, and thus to a different origin of these surfaces.

[19] In $\rho - \beta$ diagrams, β is an index in the power law distribution of quantity e, an energy expenditure per unit length of a link. The sum of e over all links in a network is the total energy dissipation in the network. One approach to study terrestrial river networks, so-called optimal channel networks models [*Rodriguez-Iturbe et al.*, 1992], assumes that the total energy dissipation is minimized by natural landscape evolution (due to rainfall-fed erosion). Indeed, such models produce networks that reproduce closely the actual river networks, having a power law distribution of e with an index of $\beta_{\mathrm{terr}} \approx 0.9$. As evident from Figure 1 there is not much difference in distribution of β between networks extracted from Noachian, Hesperian, and Amazonian terrains. In all cases $\langle\beta\rangle \approx 0.7$, although there is a wide range of individual values of β. It is interesting that the distribution of e in Martian networks is indeed a power law, albeit with an average index smaller than β_{terr}. In the terrestrial context, the power law distribution of e is interpreted as a manifestation that an evolving landscape self-organized itself into a critical state in which the energy is dissipated at all length scales. Arguably, Martian landscapes are also self-organized, however, the lower value of β indicates either a different mechanism of self-organization, or lack of critical state.

[20] Analysis of $\rho - \beta$ diagrams (bottom row on Figure 2) reveal a weak negative correlation ($r \approx -0.2$) between ρ and β for Noachian and Hesperian networks, but no correlation for Amazonian networks. Overall, $\rho - \beta$ diagrams, unlike the $\tau - \gamma$ diagrams, cannot be used as indicators of surface age. The average value of quantity ρ itself shows a certain systematic increase with decreasing surface age (see both Figures 1 and 2). This is caused by the decreasing craters count for younger surfaces. A drainage basin that embodies craters is naturally irregular and is not expected to have a high uniformity of its drainage density. For old surfaces many networks incorporate craters and the average value of ρ is relatively lower. However, the differences in the values of $\langle\rho\rangle$ between different epochs are smaller than uncertainties associated with those values, so using values of $\langle\rho\rangle$ for age determination does not appear to be practical.

5. Terrains in Different Geological Units

[21] The Martian surface is divided into geological units, terrains with common morphological features. We have

Table 1. Means and Standard Deviations of A for Terrains of Different Ages

Epoch	τ	γ	β	ρ
Noachian	0.43 ± 0.07	1.00 ± 0.22	0.70 ± 0.22	2.29 ± 0.42
Hesperian	0.44 ± 0.07	0.93 ± 0.23	0.71 ± 0.24	2.37 ± 0.44
Amazonian	0.46 ± 0.06	0.90 ± 0.18	0.72 ± 0.24	2.60 ± 0.47

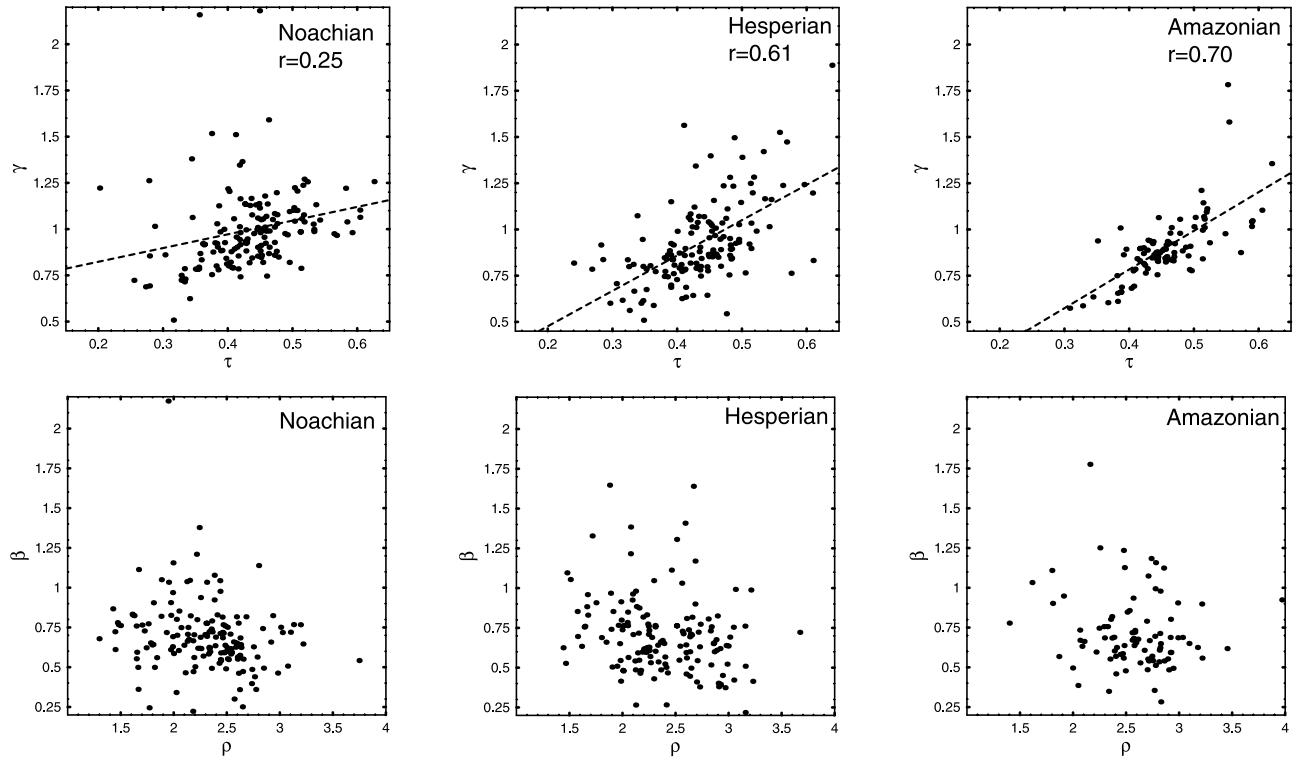

Figure 2. The network descriptors, A, for Noachian (left column), Hesperian (middle column), and Amazonian (right column) terrains. The panels in the top row show $\tau - \gamma$ diagrams that relate the two planar characteristics of the networks. The dashed line represents the best linear fit to the data, and r is the correlation coefficient. The panels in the bottom row show $\rho - \beta$ diagrams.

investigated whether the DNA method is capable of distinguishing between such units within a given epoch.

5.1. Noachian Geological Units

[22] Of 152 networks extracted from Noachian surfaces, 101 came from just three geological units. These units are: Npl1, Nplr, and Npld. The Npl1 is the most widespread highland unit with high density of craters, sparse distribution of channels, and small ridges. The Nplr is the ridged unit, moderately to heavily cratered terrain containing wide, long ridges. The Npld is the dissected unit, similar in appearance to the Npl1 unit but highly dissected by (visible) networks and small channels (all geological interpretations of the geological units are after *Tanaka and Scott* [1987]). There are 28 networks extracted from terrains contained in the Npl1 unit, 31 form the Nplr unit, and 42 from the Npld unit. The remaining 51 Noachian networks are spread over several additional geological units, small number of networks in each of these units make them unsuitable for statistical analysis.

[23] The average values and standard deviations of Noachian network descriptors are given in Table 2. These average values of A are not significantly different from each other and from $\langle A \rangle_{\mathrm{Noach}}$. Thus comparing the average values of A does not provide distinction between different geological units. Instead, some level of distinction is provided by the degree of correlation between τ and γ. Figure 3 shows the $\tau - \gamma$ and $\rho - \beta$ diagrams for networks extracted from Npl1, Nplr, and Npld geological units, respectively. For networks extracted from Npl1 terrains the $\tau - \gamma$ correlation coefficient is $r_{\mathrm{Npl1}} = 0.27$, for networks extracted from Nplr terrains $r_{\mathrm{Nplr}} = -0.17$, and for networks extracted from Npld terrains $r_{\mathrm{Npld}} = 0.41$.

[24] The Npld networks are distinguished from the rest by significantly higher value of r and higher value of $\langle \rho \rangle$. It is particularly interesting because the Npld terrains are as heavily cratered as the Npl1 terrains, and yet their networks are more "regular" as indicated by more uniform drainage density and apparent adherence to "Hack's law." Thus our DNA analysis reveals that the difference between the Npld and the Npl1 terrains is not limited to a presence of visible channel networks, but extends to an extra organization of the entire landscape.

[25] The presence of visible channel networks invites comparison between the Npld and terrestrial terrains. Figure 4 shows an example of approximately 200 km by 200 km of Npld terrain in the region of Locras Valles. The channel networks are clearly visible in this visual representation of MOLA topographic data (the left panel on Figure 4). The extracted drainage network of $\Omega = 5$ and 385 links closely follows the channel features (the right panel on Figure 4). This provides a further support that what is observed constitutes an actual drainage network. The

Table 2. Means and Standard Deviations of A for Noachian Terrains

Epoch	τ	γ	β	ρ
Npl1	0.44 ± 0.08	1.07 ± 0.27	0.69 ± 0.16	2.17 ± 0.4
Nplr	0.41 ± 0.06	1.01 ± 0.31	0.70 ± 0.17	2.20 ± 0.42
Npld	0.42 ± 0.08	0.96 ± 0.18	0.66 ± 0.18	2.38 ± 0.51

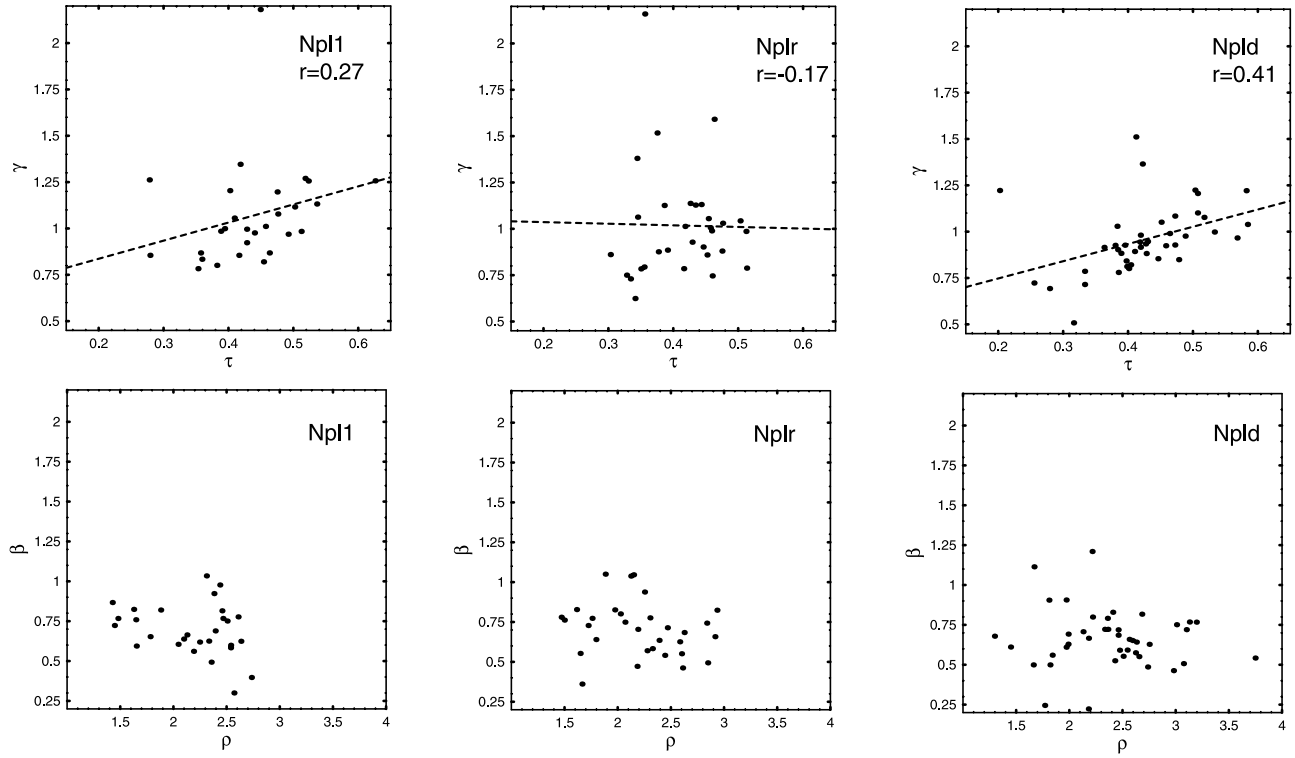

Figure 3. The network descriptors, A, for Npl1 unit (left column), Nplr unit (middle column), and Npld unit (right column) Noachian terrains. The panels in the top row show $\tau - \gamma$ diagrams that relate the two planar characteristics of the networks. The dashed line represents the best linear fit to the data, and r is the correlation coefficient. The panels in the bottom row show $\rho - \beta$ diagrams.

extracted network "looks" like terrestrial river networks and its network descriptor is $A = (0.45, 0.85, 0.55, 2.65)$.

[26] In order to examine further a similarity between terrestrial and Npld terrains we eliminated 8 networks from the original 42 Npld networks. Eliminated networks incorporated large craters and their structure were dominated by crater related features. The remaining 34 networks contain no large craters and thus reflect more closely the underlying

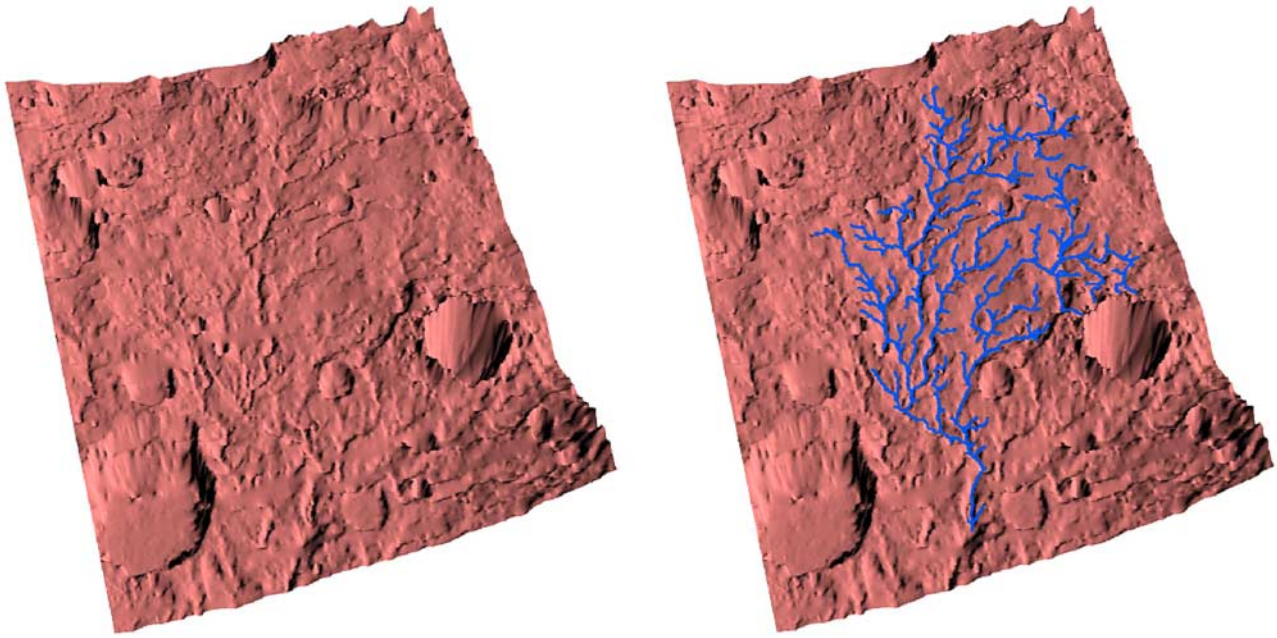

Figure 4. An example of Martian drainage network extracted from the Npld geological unit in the region of Locras Valles. On the left is a perspective view of terrain topography with exaggerated vertical dimension. On the right an extracted drainage network of $\Omega = 5$ is drawn on top of the terrain. The coordinates of the outlet are (48.27E, 9.0N), the basin drains eastward.

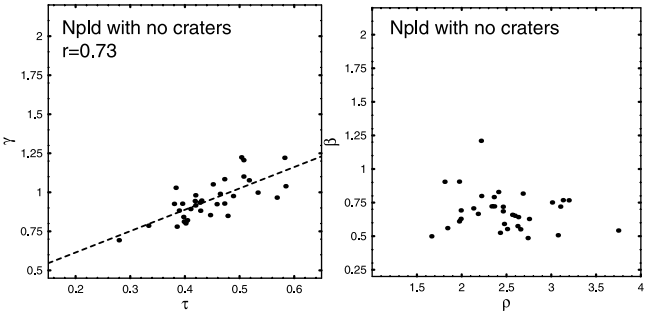

Figure 5. The network descriptors, A, for networks in the Npld unit which do not pass through large craters. The left panel shows the $\tau - \gamma$ diagram. The dashed line represents the best linear fit to the data. The right panel shows the $\rho - \beta$ diagram.

landscape morphology. The average value of the network descriptor is $\langle A \rangle = (0.44 \pm 0.07, 0.95 \pm 0.13, 0.69 \pm 0.15, 2.48 \pm 0.45)$. For comparison, the average value for terrestrial network descriptor is $\langle A_{\text{terr}} \rangle = (0.42 \pm 0.02, 0.83 \pm 0.08, 0.82 \pm 0.16, 2.90 \pm 0.36)$ [*Stepinski et al.*, 2002]. Figure 5 shows the $\tau - \gamma$ and $\rho - \beta$ diagrams for these networks. Comparison between Figures 5 and 3 (right column) shows that the Npld networks incorporating large craters were, to some degree, outliers on $\tau - \gamma$ and $\rho - \beta$ diagrams. Removing these networks significantly increases the $\tau - \gamma$ correlation to $r = 0.73$. The corresponding value of "Hack index" is $h = 0.73$.

[27] The value of h is higher than $h_{\text{terr}} \approx 0.6$ and the values of τ, γ, and ρ have broader range than their terrestrial counterparts, but the most notable difference between the Martian Npld and terrestrial networks is the systematically lower values of β for Martian networks. Thus, in comparison to their terrestrial counterparts, Martian networks dissipate relatively more energy in higher order streams (downstream). Because a planar structure of Martian Npld networks is similar to a planar structure of terrestrial networks (values of τ and γ are similar), the different distribution of energy dissipation can be directly traced to a different distribution of slopes. The mean of the local slope $|\nabla z|$ of the links of a drainage network scales with the flow rate as represented by the total contributing area a,

$$\langle |\nabla z| \rangle \propto a^{-\theta} \tag{1}$$

[28] For terrestrial river networks $\theta_{\text{terr}} \approx 0.5$. Indices θ and β can be related [*Dodds and Rothman*, 2000]

$$\theta = 1 - \frac{\tau}{\beta} \tag{2}$$

[29] Using $\langle \tau \rangle_{\text{Npld}} = 0.44$ and $\langle \beta \rangle_{\text{Npld}} = 0.69$ we obtain $\theta_{\text{Npld}} = 0.36$. Thus, in Martian networks the average slope decreases with the flow rate less than in terrestrial river networks. For example, moving along a network from a given link to a link downstream that carries 10 times as much flow, the expected slope of the downstream link is 32% of the original in a typical terrestrial network, but 44% in the Martian Npld network. This result indicates that Martian channel networks are immature or underdeveloped as compared to terrestrial river networks, they experienced relatively less erosion in the lower parts of the network. Similar conclusion has been reached by *Aharonson et al.* [2002], who reported small values of θ for Ma'adim and Al Qahira Valles on Mars.

5.2. Hesperian Geological Units

[30] Networks extracted from Hesperian surfaces belong to 5 different geological units. These units are: Hr (72 networks), Hvk (32), Had (15), Hpl3 (14), and Hh3 (12). We compare network statistics for the first three units on that list. The Hr is the ridged plains unit, moderately cratered surface, marked by long, linear to sinuous ridges. The Hvk is the knobby unit, characterized by abundant, kilometer-size, knoblike hills which are probably small volcanoes. The Had is the dissected unit, ridged plains furrowed by sinuous channels and gullies. These units lack extensive cratering and their morphologies are quite distinct. For the DNA method to be practical it should be capable of distinguishing between these units.

[31] The average values and standard deviations of Hesperian network descriptors are given in Table 3. Figure 6 summarizes the categorizing potential of the DNA method as applied to the selected three Hesperian geological units. This figure attempts to represent a spread of A for each unit. A unit is represented by an ellipsoid with a center located at $(\langle \tau \rangle, \langle \gamma \rangle, \langle \beta \rangle)$ and lengths of its semiaxes are equal to standard deviations of corresponding quantities, $(\delta\tau, \delta\gamma, \delta\beta)$. Darker shade of an ellipsoid surface indicate larger value of ρ. Thus we expect that values of A for a given unit are inside its ellipsoid. If ellipsoids for two units are disjoined the DNA method can distinguish between those units. Conjoined ellipsoids mean that unique categorization may not be possible, although values of ρ (coded by the shade of the ellipsoid surface) may provide the additional information necessary for distinction.

[32] Figure 6 indicates that the DNA method differentiates between Hr and Had geological units. Networks extracted from these two units have their network descriptors different enough for the two corresponding ellipsoids to be disjoined. Statistical properties of networks extracted from the Hvk unit show a large variation in values of components of the network descriptor from one network to another. This variability translates into a large ellipsoid that intersects with ellipsoids for Hr and Had units. As a result there are some values of (τ, γ, β) that can indicate either the Hr or the Hvk terrain. Likewise some values of (τ, γ, β) may indicate either the Had or the Hvk terrain. However, the Hvk networks are characterized by high values of ρ, so, overall, the DNA method is capable of differentiating between these three Hesperian units.

[33] Because Hesperian surfaces are not heavily cratered, values of τ and γ are highly correlated, $r_{\text{Hr}} = 0.7$, $r_{\text{Hvk}} =$

Table 3. Means and Standard Deviations of A for Hesperian Terrains

Epoch	τ	γ	β	ρ
Hr	0.43 ± 0.07	0.99 ± 0.23	0.73 ± 0.21	2.22 ± 0.36
Hvk	0.46 ± 0.07	0.84 ± 0.24	0.67 ± 0.28	2.8 ± 0.36
Had	0.39 ± 0.06	0.76 ± 0.13	0.51 ± 0.11	2.34 ± 0.29

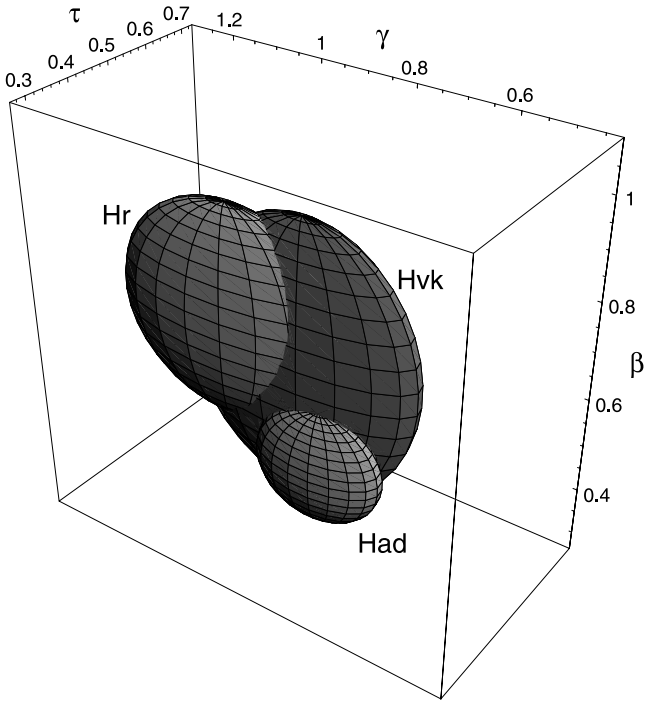

Figure 6. Typical values of network descriptors for Hesperian geological units, Hr, Hvk, and Had as represented by ellipsoids in the (τ, γ, β) space. The center of an ellipsoid representing a given unit is located at ($\langle\tau\rangle$, $\langle\gamma\rangle$, $\langle\beta\rangle$), and lengths of its semi-axes are equal to standard deviations of corresponding quantities, ($\delta\tau$, $\delta\gamma$, $\delta\beta$). The larger value of $\langle\rho\rangle$ is indicated by darker surface of an ellipsoid.

0.78, and $r_{\mathrm{Had}} = 0.59$. Because of this high correlation "Hack's law" applies, and values of an index h are: $h_{\mathrm{Hr}} = 0.44$, $h_{\mathrm{Hvk}} = 0.40$, $h_{\mathrm{Had}} = 0.82$.

5.3. Amazonian Geological Units

[34] We have extracted 89 networks from Amazonian geological units, There are 38 networks from terrains in the Apk unit, 26 in the Aps unit, 14 in the Aoa unit, and 10 in the Ael unit. We compare network statistics for the first three units on that list. The Apk is the knobby unit, generally smooth plains with conical hills or knobs. The Aps is the smooth, sparsely cratered unit. The Aoa unit encompasses aureole deposits surrounding Olympus Mons. Visually, the morphologies of Apk and Aps terrains are not strikingly different, but the morphology of the Aoa terrains is very distinct.

[35] The average values and standard deviations of Amazonian network descriptors are given in Table 4. Figure 7 summarizes the categorizing potential of the DNA method as applied to these Amazonian geological units. This is the same type of figure as Figure 6. The ellipsoids for Apk and Aps units intersect significantly. Although the Apk unit is characterized by higher value of $\langle\rho\rangle$, there is a significant subset of the parameter space for which the DNA method cannot distinguish between the two terrains. The ellipsoid for the Aoa unit is rather large due to large variation in the values of β. Again, there is an intersection between Aoa ellipsoid and the ellipsoids for the other two units, so distinction on the basis of (τ, γ, β) alone is not always possible. However, the high values of ρ for the Aoa networks provides additional distinction. For Amazonian terrains values of τ and γ are highly correlated, $r_{\mathrm{Apk}} = 0.6$, $r_{\mathrm{Aps}} = 0.76$, and $r_{\mathrm{Aoa}} = 0.94$. The values of the Hack's index are: $h_{\mathrm{Apk}} = 0.57$, $h_{\mathrm{Aps}} = 0.38$, $h_{\mathrm{Aoa}} = 0.52$.

Table 4. Means and Standard Deviations of A for Amazonian Terrains

Epoch	τ	γ	β	ρ
Apk	0.47 ± 0.06	0.92 ± 0.17	0.67 ± 0.18	2.67 ± 0.36
Aps	0.45 ± 0.07	0.94 ± 0.23	0.76 ± 0.21	2.32 ± 0.39
Aoa	0.45 ± 0.07	0.84 ± 0.14	0.81 ± 0.37	2.94 ± 0.67

[36] Thus the DNA method can differentiate between the Aoa and the either Apk or Aps terrains. The unit Aoa (Olympus Mons aureole) stands out for several reasons. This unit has the highest $\tau - \gamma$ correlation observed on Mars; thus it is the unit that most closely observes a Hack's law relationship. Unit Aoa also has some of the highest observed values of ρ on Mars. These attributes, taken out of geological context, could suggest highly eroded, "terrestrial-like" surface. However, unit Aoa is known to contain some of the roughest terrain on the planet on both 100-m [*Smith et al.*,

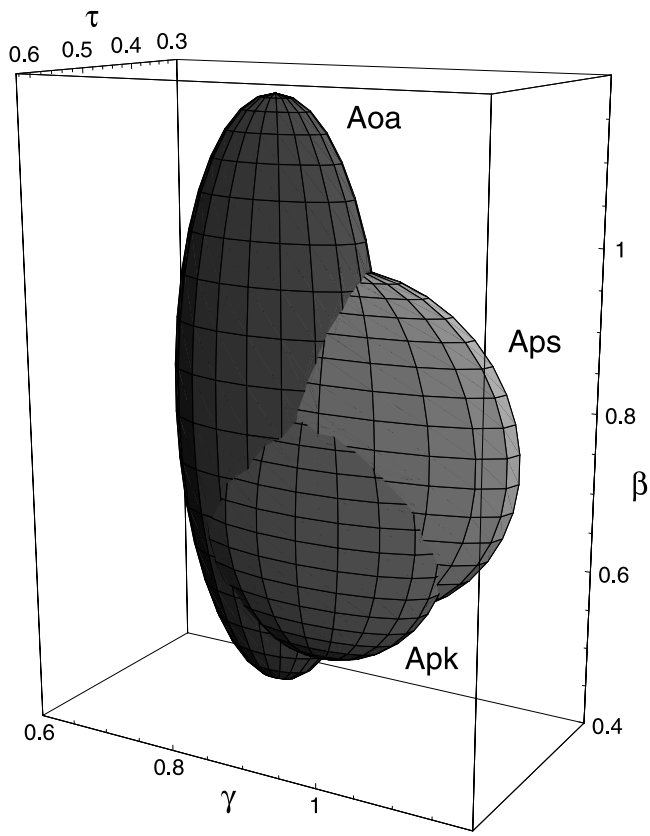

Figure 7. Typical values of network descriptors for Amazonian geological units, Apk, Aps, and Aoa as represented by ellipsoids in the (τ, γ, β) space. The center of an ellipsoid representing a given unit is located at ($\langle\tau\rangle$, $\langle\gamma\rangle$, $\langle\beta\rangle$), and lengths of its semi-axes are equal to standard deviations of corresponding quantities, ($\delta\tau$, $\delta\gamma$, $\delta\beta$). The larger value of $\langle\rho\rangle$ is indicated by darker surface of an ellipsoid.

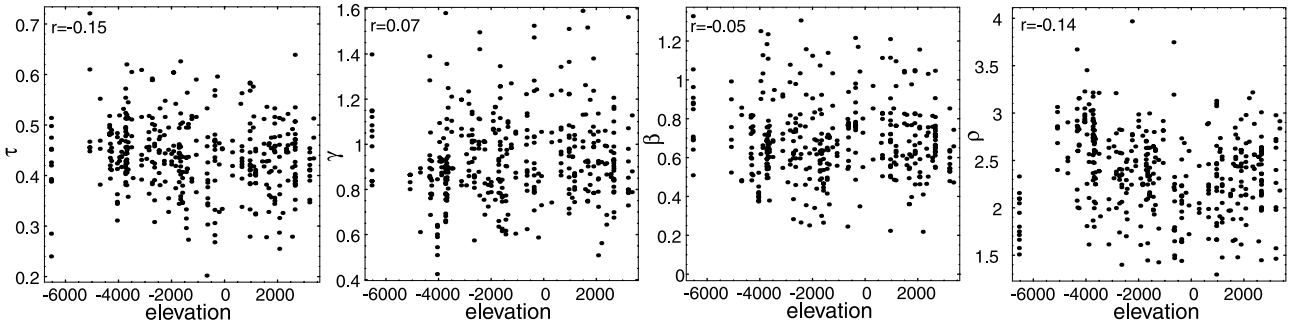

Figure 8. Scatter plots of elevation (in meters) versus components of network descriptor. All 387 networks are shown, values of the correlation coefficient are given in the upper left corner of each panel.

2001] and regional scales [*Aharonson et al.*, 2001], distinctively non-terrestrial surface properties. Recall from section 2 that an observance of Hack's law indicates landscape organization, and high values of ρ indicates landscape homogeneity. Often the landscape is organized and homogenous because it is highly eroded. The unit Aoa is an example of a rough landscape that, nevertheless, is homogeneous and organized.

6. Dependence on Elevation and Geographical Location

[37] The 74 Martian locations that we investigate in this paper are located at very different elevations ranging from −6500 m to +3300 m. By "location" we understand a section of the Martian surface represented by a single DEM. A characteristic surface area of our locations is relatively large at about 10^5 km^2. There are typically several drainage networks extracted from a single location. Because we want to investigate a potential large-scale dependence of landscape morphology (as encapsulated by network descriptors) on elevation, all networks from a single location are assigned the same value of elevation equal to an average over a given location.

[38] In principle, the Martian climate, and thus erosional process, could depend on elevation [*Craddock and Maxwell*, 1993], and it is interesting to check for potential correlations between an elevation and components of the network descriptor. Figure 8 shows scatter plots relating components of A to elevation for all 387 drainage networks. It is clear that these components appear to be independent from the elevation, the full range of values for each component can be found at any elevation. This conclusion is formalized by calculating correlation coefficients that are all close to zero. Constructing similar scatter plots for a subset of networks restricted to a single age epoch does not change the no-correlation conclusion.

[39] We have also investigated a potential dependence of network descriptor on geographical region. Our topographical data come from 25 large-scale named geographical regions. Typically we have several DEMs (locations) extracted from any single region. Because Martian topography can, in principle, be influenced by local factors, we looked at dependence of values of components of A on regions. Figure 9 shows plots relating components of A to regions for all 387 drainage networks. The regions have been numbered from 1 to 25 in decreasing order of number of extracted networks. In addition, for each region we also plot mean values and the standard deviation bounded ranges of components of A. Although mean values of components of A change from one region to another, the changes are typically within bounds of a standard deviation.

[40] Finally, we have studied a dependence of components of A on location's latitude. No significant correlation was found. Overall, we have concluded that the DNA method shows no regional trends in Martian terrain morphology.

7. Discussion and Conclusions

[41] Our long term goal is to develop an algorithmic method for morphological characterization and classification of Martian landscapes on the basis of topographical

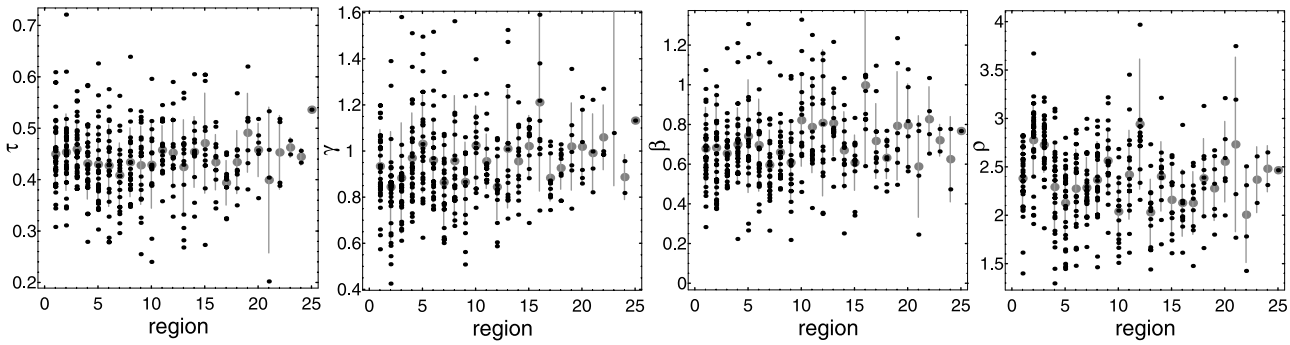

Figure 9. Plots of regions versus components of network descriptor. The regions have been numbered from 1 to 25 in decreasing order of number of extracted networks. All 387 networks are shown. Gray points indicate a region-averaged values and the gray vertical bars represent standard deviations.

data. Presently, such a classification is based on a natural language description. Automated characterization is meant to complement rather than to replace descriptive schemes such as Martian geological units. A computer procedure has an advantage of producing results that are objective and quantitative, but it may have difficulties recognizing some geomorphologic features that are immediately apparent to an expert. Thus we envision applying algorithmic classifier for studies where a global comparison is called for, but probably not for studies that focus on details of a particular location.

[42] In this paper we have proposed and investigated a particular algorithmic landscape characterization method based on the idea that terrains of different morphologies drain in different patterns. We emphasize that our method is applied to arbitrarily chosen surfaces, and is not restricted to surfaces that have been actually subject to fluvial erosion. Thus our proposed method, the DNA method, uses characterization and classification of drainage networks as a proxy for characterization of landscapes. Drainage networks, readily extracted from a landscape, are 3-dimensional structures having fractal geometry. The overall character of a network is encapsulated in the network descriptor, a short summary of how various drainage properties are distributed over the network. The bulk of our analysis was devoted to establish whether Martian landscapes could be characterized in terms of network descriptors.

[43] The mean value of a Martian network descriptor, averaged over all 387 networks that we have extracted, is $\langle A \rangle_{\mathrm{Mars}} = (0.44 \pm 0.07, 0.95 \pm 0.22, 0.71 \pm 0.23, 2.39 \pm 0.45)$ This could be compared to the mean value of a Martian network descriptor, averaged over 20 networks, calculated previously by *Stepinski et al.* [2002], $\langle A \rangle_{\mathrm{Mars}}^{\mathrm{prev}} = (0.44 \pm 0.02, 0.87 \pm 0.06, 0.68 \pm 0.09, 2.99 \pm 0.32)$. There is no more than 8% difference between individual components of the two mean Martian network descriptors. However, the networks extracted in the present study show larger variation in the component values of the network descriptor as evident by significantly larger values of standard deviations. This is partially due to the fact that networks considered by *Stepinski et al.* [2002] are all relatively extensive, with a minimum value of Ω equal to 5. If we restrict our present sample to networks with $\Omega \geq 5$, the mean network descriptors changes very little, but standard deviations of its components decrease. However, they are still larger than in the study of *Stepinski et al.* [2002]. We attribute this remaining difference to the fact that most of the networks in the previous study were extracted from terrains showing visual evidence of channels, whereas networks in the present study were extracted without any visual guidance.

[44] We have found that there is a significant scatter in values of network descriptors even for networks extracted from the same geological unit. This is not particularly surprising because significant scatter is measured in values of terrestrial network descriptors characterizing networks incised by a single erosional process. The classification of networks (and thus landscapes) on the basis of network descriptors becomes difficult if the scatter in values of A becomes comparable to the actual values of A. This is often the case for Martian networks, and, consequently, in most cases, a descriptor of a single network cannot uniquely determine an epoch or/and geological unit of a terrain from which it was extracted. Nevertheless the DNA method can distinguish between different terrains, but in a statistical, rather than an individual sense. Thus a distinction between two landscapes of different morphology is provided not by contrasting the two representative networks, but rather by contrasting the statistics of two representative collections of networks.

[45] The statistics of A can be used to measure the degree of surface cratering and thus, indirectly, to determine the surface's age. In section 4 we have demonstrated that the degree of correlation between values of τ and γ corresponds to crater count. Interestingly, this is the correlation between these two quantities, and not the actual distributions of their values that provides the measure of cratering. We suggest that the DNA method offer a potentially interesting alternative to crater count as an age determining technique. A calibration between the correlation coefficient and the age needs to be established which is beyond the scope of this paper. Further work is needed to assess suitability of the DNA method for surface's age determination.

[46] The ability of the DNA method to recognize geological units depends on the degree of cratering. The method is very sensitive to the presence of craters, and for heavily cratered terrains the signature of features such as, for example, presence or absence of ridges or channels, is hidden by a stronger signature of craters presence. However, for surfaces that are not heavily cratered, the DNA method can statistically distinguish between different Martian geological units. In sections 5.2 and 5.3 we have demonstrated how networks from different geological units have their network descriptors preferentially located at different segments of the four-dimensional A-space. This suggests two possible procedures for an algorithmic identification of a geological unit associated with a given terrain. One possibility is to extract a single network from a terrain in question and to compare its network descriptor to a set of network descriptors expected for a particular geological unit. One possible definition of an "expected set" is given in section 5.2 in the form of "expectancy" ellipsoids shown on Figures 6 and 7. Using such a procedure we can calculate a likelihood that a terrain belongs to a specific geological unit. The second possibility is to extract a collection of networks from a given terrain and to construct an expectancy ellipsoid. In this case an identification is achieved by comparison of such an ellipsoid to templates constructed for specific geological units.

[47] Our findings exposed several practical difficulties with the concept of using characterization and classification of drainage networks as the means for an automated characterization and classification of landscapes. We have found that although visually different landscapes have indeed visually different drainage networks, it is sometimes difficult to connect differences in networks' visual appearances with differences in values of their network descriptors. Perhaps, this is because the network descriptor consist of quantities that are "high level" features (indices of the power law distributions) that relate to network's appearance in an indirect fashion. More work is needed to understand better the relation between A and a visual appearance of a network.

[48] Although the primary focus of this paper was to investigate the possibility of algorithmic classification of

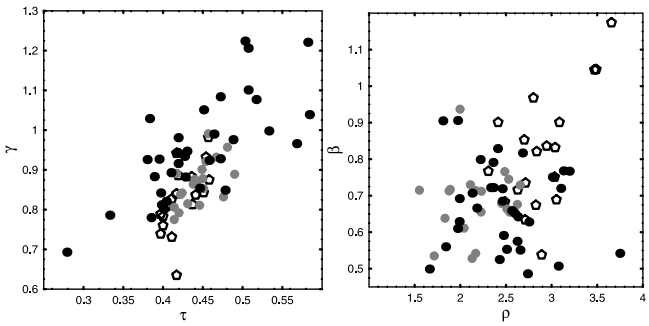

Figure 10. The network descriptors, A, for networks in the Npld unit which are not dominated by craters (black dots), Martian networks extracted by *Stepinski et al.* [2002] (gray dots), and selected terrestrial networks (open pentagons). The left panel shows the $\tau - \gamma$ diagram and the right panel shows the $\rho - \beta$ diagram.

Martian landscapes using the DNA method, our data can also be used for a quantitative characterization of Martian valley networks. Features reminiscent of terrestrial river networks are visible on orbital images of some, mostly Noachian Martian surfaces. The descriptive morphology of these networks has been used [*Pieri*, 1980; *Squyres and Kasting*, 1994] to argue for or against particular processes responsible for the observed structures. Focusing on locations displaying prominent valley networks, *Stepinski et al.* [2002] extracted 20 drainage networks from MOLA topography. Extracted networks follow closely the visual network-like features, reinforcing the notion that what is observed is actually a drainage network. The database created for the present work contains 42 networks extracted from surfaces classified as Npld, a Noachian terrain highly dissected by channels presumably produced by rain-water runoff or groundwater sapping [*Craddock and Maxwell*, 1993]. Unlike in the study by *Stepinski et al.* [2002], the Npld terrains have not been chosen for presence of prominent, highly integrated valley networks, and the drainage networks have not been extracted to specifically follow any visible feature. Interestingly, a comparison of network descriptors of drainage networks extracted by *Stepinski et al.* [2002] (selected to follow prominent, highly integrated fluvial features) and network descriptors of drainage networks extracted from the Npld terrains (selected randomly) show a remarkable similarity.

[49] Figure 10 shows the $\tau - \gamma$ and $\rho - \beta$ diagrams for these two samples of networks. The Npld sample is restricted to 34 networks which are not dominated by craters (see section 5.1). In addition, data for 19 terrestrial river networks are also plotted on Figure 10. The $\tau - \gamma$ diagram reveals that in both samples τ and γ are correlated to approximately the same degree, $r \approx 0.7$ for the Npld sample and $r \approx 0.6$ for the *Stepinski et al.* [2002] sample. Moreover, the best linear fit to the (τ, γ) data yields the slope of 1.37 for the Npld sample and 1.5 for the *Stepinski et al.* [2002] sample. The only clear difference between the two samples is the range of values. In particular, there are 8 Npld networks with $\tau > 0.5$, these turn out to be relatively smaller networks. There are also 2 Npld networks with $\tau < 0.35$, these turn out to incorporate a sizable crater into their structure (even so the networks in the sample were selected not to be dominated by craters). Overall, The planar character of the samples (degree of correlation and the slope of linear relation) is remarkably similar. The sample of terrestrial river networks has a similar degree of correlation ($r = 0.61$), but a different slope of the best linear fit to the (τ, γ) data (2.31). The $\rho - \beta$ diagram again shows that both samples occupy approximately the same region of the (ρ, β) space, although the some networks in the Npld sample have higher values of β, again, these are relatively smaller networks. Overall, we conclude that the DNA description of the Npld terrains is statistically identical to the DNA description of terrains with prominent valley networks. This indicates that the morphology of the Npld terrain is, on the fundamental level, identical to the morphology of the terrain with prominent valley networks, even if no clearly defined networks are visible. This suggests that the Npld terrain that do not show prominent and integrated fluvial features, nevertheless experienced the same erosional process as the terrain displaying prominent channel networks. The lack of integrated networks may be due to subsequent roughening processes affecting different sites to a different degree.

[50] Interestingly, the statistics of A for all Npld terrains differs in two features from the statistics of A for terrestrial terrains. First, the slope of the best-fit linear relation between τ and γ is smaller for the Npld terrains than it is for the terrestrial terrains. In other words, the Npld drainage networks obey Hack's law, but the value of an index h is larger for Martian networks. This result needs further corroboration by calculating the value of h using more robust technique, such as analysis of the scaling of the moments of stream lengths distribution [*Rigon et al.*, 1996]. Second, the values of β are smaller for Martian networks. This result has been discussed in section 5.1 and attributed to erosional immaturity of Martian terrain. One plausible explanation is that the Martian terrain experienced only a limited amount of rainfall, enough to incise channels, but not enough to imprint a terrestrial-like slope distribution.

[51] **Acknowledgments.** This research was conducted at the Lunar and Planetary Institute, which is operated by the Universities Space Research Association under contract CAN-NCC5-679 with the National Aeronautics and Space Administration. This is Lunar and Planetary Institute Contribution No. 1189.

References

Aharonson, O., M. T. Zuber, and D. H. Rothman (2001), Statistics of Mars' topography from the Mars Orbiter Laser Altimeter: Slopes, correlations, and physical models, *J. Geophys. Res.*, *106*, 723–735.

Aharonson, O., M. T. Zuber, D. H. Rothman, N. Schorghofer, and K. X. Whipple (2002), Drainage basins and channel incisions on Mars, *Proc. Natl. Acad. Sci. U. S. A.*, *99*(4), 1780–2783.

Carr, M. H., and G. D. Clow (1981), Martian channels and valleys: Their characteristics, distribution, and age, *Icarus*, *48*, 91–117.

Craddock, R. A., and T. A. Maxwell (1993), Geomorphic evolution of the Martian highlands through ancient fluvial processes, *J. Geophys. Res.*, *98*, 3453–3468.

Dodds, P. S., and D. H. Rothman (2000), Scaling, universality, and geomorphology, *Annu. Rev. Earth Planet. Sci.*, *28*, 571–610.

Gershenfeld, N. (1999), *The Nature of Mathematical Modeling*, Cambridge Univ. Press, New York.

Hack, J. T. (1957), Studies of longitudinal profiles in Virginia and Maryland, *U.S. Geol. Surv. Prof. Pap.*, *294-B*, 45–97.

Horton, R. E. (1945), Erosional development of streams and their drainage basins: Hydrophysical approach to quantitative morphology, *Bull. Geol. Soc. Am.*, *56*(3), 275–370.

Pieri, D. C. (1980), Martian valleys: Morphology, distribution, age, and origin, *Science*, *210*, 895–897.

Rigon, R., I. Rodriguez-Iturbe, A. Maritan, A. Giacometti, D. G. Tarboton, and A. Rinaldo (1996), On Hack's law, *Water Resour. Res.*, *32*(11), 3367–3374.

Rinaldo, A., I. Rodriguez-Iturbe, and R. Rigon (1998), Channel networks, *Annu. Rev. Earth Planet. Sci.*, *26*, 289–327.

Rodriguez-Iturbe, I., and A. Rinaldo (1997), *Fractal River Basins: Chance and Self-Organization*, Cambridge Univ. Press, New York.

Rodriguez-Iturbe, I., A. Rinaldo, R. Rogon, R. L. Bras, and E. Ijjasz-Vasquez (1992), Energy dissipation, runoff production and the three dimensional structure of channel networks, *Water Resour. Res.*, *28*(4), 1095–1103.

Scott, D. H., and M. H. Carr (1977), Geological map of Mars, *U.S. Geol. Surv. Misc. Geol. Invest. Ser.*, *Map I-1093*.

Smith, D. E., et al. (2001), Mars Orbiter Laser Altimeter: Experiment summary after the first year of global mapping of Mars, *J. Geophys. Res.*, *106*, 23,689–23,722.

Squyres, S. W., and J. F. Kasting (1994), Early Mars: How warm and how wet?, *Science*, *265*, 744–749.

Stepinski, T. F., M. M. Marinova, P. J. McGovern, and S. M. Clifford (2002), Fractal analysis of drainage basins on Mars, *Geophys. Res. Lett.*, *29*(8), 1189, doi:10.1029/2002GL014666.

Tanaka, K. L., and D. H. Scott (1987), Geological map of the polar regions on Mars, *U.S. Geol. Surv. Misc. Geol. Invest. Ser.*, *Map I-1802-C*.

Tarboton, D. G., R. L. Bras, and I. Rodriguez-Iturbe (1988), The fractal nature of river networks, *Water Resour. Res.*, *24*(8), 1317–1322.

Tarboton, D. G., R. L. Bras, and I. Rodriguez-Iturbe (1989), The analysis of river basins and channel networks using digital terrain data, *Tech. Rep. 326*, Ralf M. Parsons Lab., Mass. Inst. of Technol., Cambridge.

Tarboton, D. G., R. L. Bras, and I. Rodriguez-Iturbe (1991), On the extraction of channel networks from digital elevation data, *Hydrol. Processes*, *5*(1), 81–100.

Wessel, P., and W. H. F. Smith (1991), Free software helps map and display data, *Eos Trans. AGU*, *72*, 441.

S. M. Clifford, P. J. McGovern, and T. F. Stepinski, Lunar and Planetary Institute, 3600 Bay Area Boulevard, Houston, TX 77058, USA. (tom@lpi.usra.edu)

M. L. Collier, Department of Earth Science, Rice University, Houston, TX 55005, USA. (spaceman@rice.edu)